

Experimental And Numerical Analysis Of Air-Water Separation Efficiency Using A Cavity Separator

Panopoulos A. Nikolaos

Mechanical Engineering and Aeronautics Dept.
University of Patras
Patras, Greece
panopoulos@mech.patras.gr

Margaris P. Dionissios

Mechanical Engineering and Aeronautics Dept.
University of Patras
Patras, Greece
margaris@mech.upatras.gr

Abstract— The recirculating air vortex that is formed in the street canyon phenomenon is the principle operation idea for the experimental and numerical investigation of a new mixture separator. Air-water mixture flow experiments were executed in one orthogonal pipe 1500mm long with a cross section of 25mm x 55mm. Three symmetrical cavities (55 x 55 x 55mm) were placed at the front surface of the duct. In order to optimize the system separation efficiency value, a series of CFD simulations were executed. A wide range of phase mixing percentage is covered. The numerical two-phase flow process simulation carried out using FLUENT 16 combined with the VOF multiphase model. The results are presented in terms of air separation efficiency and air volume fraction distribution. Moreover, the observed experimental flow patterns are compared with the numerical volume fraction contours. The analysis of the results delimits the areas of best performance of this initial separator design.

Keywords—air separation efficiency; mixture separator; street canyon phenomenon; two phase flow; flow pattern;

I. INTRODUCTION

Interesting multiphase flows occur inside pipes and applications of nuclear industry, in hydrocarbon extraction and in chemical engineering. The most common multiphase flows in petrochemical applications are liquid-liquid (e.g. oil extraction) or gas – liquid in evaporation or absorption. In multiphase flow studies a practical and low cost way to separate mixtures is under investigation. In most cases due to the limitation of the conditions and process equipment a mixture separator must be efficient, easily maintained, in compact size and adjustable to many geometries [1]. The most common mixture separator in industry and in literature is the T-junction [2], [3]. Significant research effort has been focused on gas/liquid flow [4], [5] and on liquid-liquid flow inside a T- Junction [6], [7].

In this study a novel air-water separator is validated numerically based on the experimental results of a previous study [8]. The separation mechanism is based on the street canyon phenomenon. According to Vardoulakis et al. [9] the street canyon is a relatively

narrow street with buildings lined up continuously along both sides. The street canyon phenomenon is the recirculating air vortex inside the cavity that is formatted between the buildings in an urban area [9].

The air trapping mechanism has been examined experimentally and numerically by Panopoulos et al. [10-13]. The results indicate that the cavity separator can be used to separate mixtures of fluids with different densities. Only horizontal flow separation has been examined up to now.

The magnitudes of interest are presented in terms of air separation efficiency (α_{air}) and air volume fraction (ϵ_{air}). Moreover, the superficial velocities of the water (J_w) and of the air (J_g) are used for convenience.

II. EXPERIMENTAL INSTALLATION AND PROCEDURE

The experimental apparatus was designed and manufactured for air-water flow in the Fluid Mechanics Laboratory, at the Mechanical Engineering and Aeronautics Department at the University of Patras. The experimental system is presented in Figure 1. The test section pipe was made of Plexiglas for flow visualization purposes. The basic instrumentation is listed: 1) Water tank, 2) Water pump, 3) Test section, 4) Water rotameter, 5) Air rotameter, 6) Pressure manometer, 7) Water valve, 8) Mixture T-junction, 9) Air collector, 10) Air flowmeter, 11) Cavity separator and 12) Air compressor.

In the experimental system the tank is filled with water at atmospheric pressure. The pump supplies the water to the water rotameter and the flow rate is adjusted with two valves. At the same time the air compressor supplies the air. When the compressed air is supplied its pressure and temperature are listed at the inlet point with two transducers. There are two air rotameters with different scales, one with a range 1 – 14 L/min and the second with range 10 – 150 L/min. The air supply is regulated with the proper valve. The equations that were used to export numerical results are:

$$Q = Q_0 \cdot \sqrt{\frac{\rho \cdot T \cdot P_0}{\rho_0 \cdot T_0 \cdot P}} \quad (1)$$

where Q is the real air volume flow rate and ρ , T, P the density, temperature, and pressure of air. The subscript 0 defines operating conditions while the

magnitudes without subscript are referred to normal conditions.

The efficiency of the separation mechanism is defined as:

$$a = \frac{Q_{air,out}}{Q} \quad (2)$$

where $Q_{air,out}$ is the sum of volume flow rate of air from each cavity and Q is the volume flow rate of air that is supplied at entry in normal conditions, with Q as defined in Eq.1. The void fraction (or volume fraction) of air is defined as:

$$\varepsilon_{air} = \lim_{\delta V \rightarrow 0} \frac{\delta V_{air}}{\delta V} \quad (3)$$

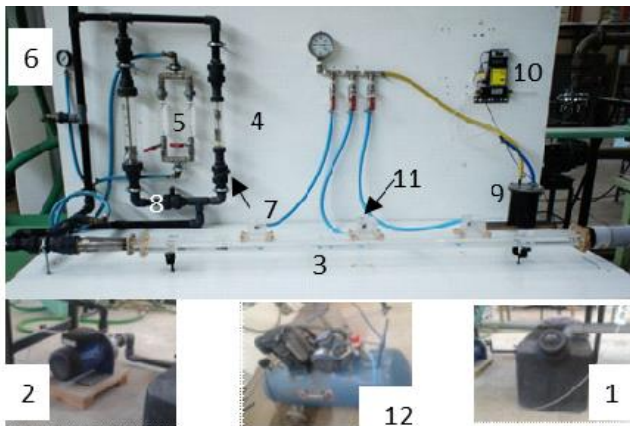


Fig. 1: Experimental Facility

III. CFD INVESTIGATION

The computational analysis was carried out with Ansys Fluent 16 [14]. This commercial software package is widely used for mixture flow simulations. Three computational grids were tested and the one consisted of 225,000 hexahedral cells was used. The geometry domain is a pipe with a cross sectional area of 25 x 55mm and 1500mm long. Each cavity is 55mm width and the distance between the cavities is 388.75mm. The first cavity is fitted 33.75mm from the two phase mixing inlet point. The cavity-outlets are located on the top surface of each cavity ($\varnothing 20$).

The boundary conditions that were selected for the numerical simulations are: velocity inlets, one for each phase, three cavity pressure outlets and the main outlet of the pipe. More analytically the experimental geometry domain is presented by Zoga et al. [8].

A. Turbulence Model

The Standard k- ε viscous model was selected for Fluent simulations. The turbulence kinetic energy, k , and its dissipation rate, ε , are obtained from the following transport equations [14].

$$\frac{\partial}{\partial t}(\rho\varepsilon) + \frac{\partial}{\partial x_i}(\rho\varepsilon u_i) = \frac{\partial}{\partial x_j} \left[\left(\mu + \frac{\mu_t}{\sigma_\varepsilon} \right) \frac{\partial \varepsilon}{\partial x_j} \right] + C_{1\varepsilon} \frac{\varepsilon}{k} (P_k + C_{3\varepsilon} P_b) - C_{2\varepsilon} \rho \frac{\varepsilon^2}{k} + S_\varepsilon \quad (4)$$

This requires a dissipation rate, ε , which is entirely modeled phenomenologically as follows:

$$\frac{\partial}{\partial t}(\rho\varepsilon) + \frac{\partial}{\partial x_i}(\rho\varepsilon u_i) = \frac{\partial}{\partial x_j} \left[\left(\mu + \frac{\mu_t}{\sigma_\varepsilon} \right) \frac{\partial \varepsilon}{\partial x_j} \right] + C_{1\varepsilon} \frac{\varepsilon}{k} (P_k + C_{3\varepsilon} P_b) - C_{2\varepsilon} \rho \frac{\varepsilon^2}{k} + S_\varepsilon \quad (5)$$

B. Multiphase Model

The air-water flow regime is simulated with the Volume of Fluid (VOF) multiphase model. The VOF is a Euler-Euler approach for multiphase flow calculation. The VOF model is applied on a fixed Eulerian mesh and is designed for two or more fluids and the interface between the two fluids is of interest. Some of its applications are the motion of large bubbles in a liquid or the transient tracking of any liquid-gas interface. It solves a set of n momentum equations for each phase [14].

Geo-Reconstruct scheme is best suited for volume fraction, PISO algorithm is used for the Pressure-Velocity coupling and PRESTO interpolation scheme is used for pressure since gravity is the predominant force acting on the flow. Every other spatial discretization scheme is second order for precision issues while for the accuracy of the solutions, a value of 10^{-4} is used for all residual terms.

The water-liquid was selected as primary and the air was the secondary phase. The water has density $\rho_w = 998.2 \text{ kg/m}^3$ and viscosity $\mu_w = 0.001003 \text{ kg/m}\cdot\text{s}$. The air has density $\rho_{air} = 1.225 \text{ kg/m}^3$ and viscosity $\mu_{air} = 1.7894\text{e-}05 \text{ kg/m}\cdot\text{s}$.

For each simulation a "Flow rate (kg/s) – Flow time (s)" chart is plotted. The simulation is stopped when the values of the flowrate from the cavity – outlets are stabilized to an almost constant value. An example is presented in Figure 2.

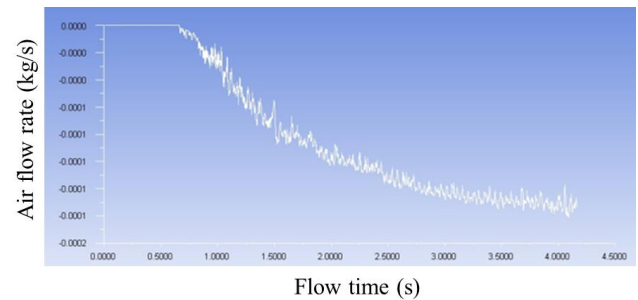


Fig. 2: Air mass flow rate (kg/s) (Fluent)

IV. RESULTS

The 3D examined numerical simulations include air and water mixture flow for 1, 2 and 3 m^3/h water volume rates. In each case the water flow rate is constant and the air flow rate is increased gradually from 1.3 to 18.3 m^3/h .

In Figures 3, 4 and 5 the volume fraction of air is presented. These three figures present the distribution of the two phases for the best air separation efficiency. In all cases the separation is high when both superficial velocities are low. This means that when the two phases flow without high slip velocity the separation level increases. It can be also observed that the water volume fraction increases as the water volume rate is higher and occupies more

percentage of the cross sectional area. In Figure 3 the mixing boundary conditions are: Water velocity $J_w = 0.2$ m/s and air velocity $J_G = 0.3$ m/s.

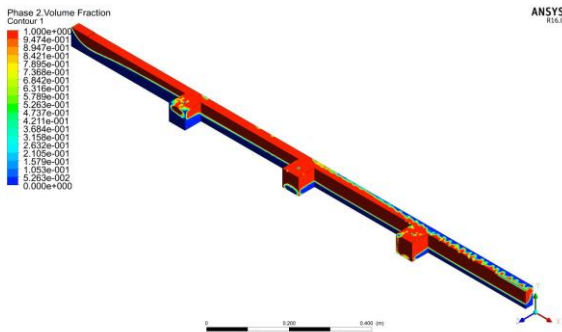


Fig. 3: Flow pattern for best separation case ($Q_w: 1\text{m}^3/\text{h}$)

In Figure 4 the mixing boundary conditions are: Water velocity $J_w = 0.4$ m/s and air velocity $J_G = 0.3$ m/s.

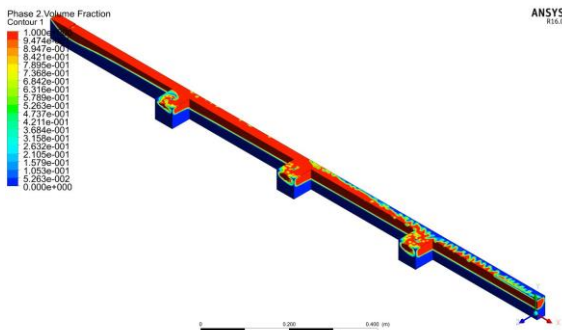


Fig. 4: Flow pattern for best separation case ($Q_w: 2\text{m}^3/\text{h}$)

In Figure 5 the mixing boundary conditions are: Water velocity $J_w : 0.6$ m/s and air velocity $J_G: 0.3$ m/s.

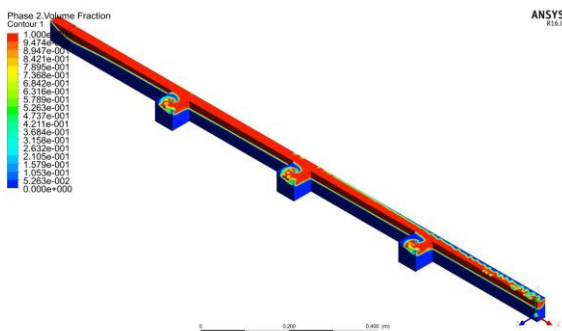


Fig. 5: Flow pattern for best separation case ($Q_w: 3\text{m}^3/\text{h}$)

The stratified, wavy, plug and bubble flow patterns are observed in all simulations. The transition occurs as the air velocity increases. At first the stratified flow is formatted. Secondly small waves are created and when the velocities are high, small air bubbles travel in the liquid domain.

The streamlines of the air phase show the “street canyon” phenomenon [9, 15]. The street canyon effect is the main idea for the construction of this mixture separator. The negative effect of the air/solid/pollutant trapping mechanism inside the urban canyons is used to separate the mixture. The geometry with the symmetric cavity forces the air inside the desired

region [9]. The pressure difference due to the high velocity inside the cavity and the density difference lead the air to exit the geometry domain through the outlet which is circular ($\varnothing 20$).

In Figure 6 the air vortices inside the three cavities are obvious. The interesting conclusion is that the three cavities contribute with different way to the total separation. The first cavity forces more air quantity to exit the test section. However, the air occupies only the upper part of the cavity. The air distribution inside the third cavity is different. The air has lost kinetic energy and the cavity cannot separate efficiently the mixture.

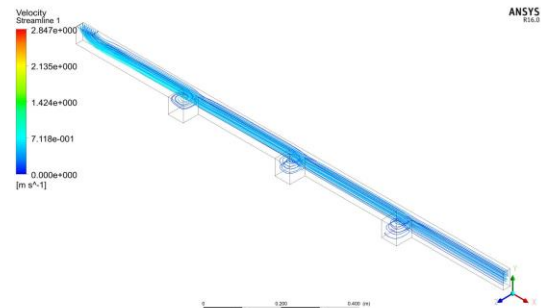


Figure 6: Air streamlines for $Q_w: 1\text{m}^3/\text{h}$

In Figure 7 the streamlines of air are presented for the second water flow rate ($Q_w: 2\text{m}^3/\text{h}$). The distribution of air in this case inside the cavities seems to be more uniform than the one observed in Figure 6.

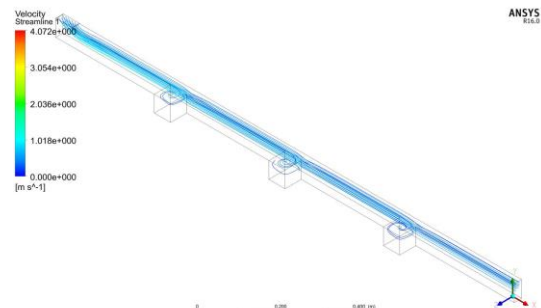


Fig. 7: Air streamlines for $Q_w: 2\text{m}^3/\text{h}$

In Figure 8 the superficial velocity of the water is 0.6 m/s. The duct is filled with more water than the previous cases. As a result, the free cross sectional area of the pipe for the air is less. In addition to that the third cavity traps less air quantity of air. No stream lines can be observed inside the cavity so that means that the air velocity is too low.

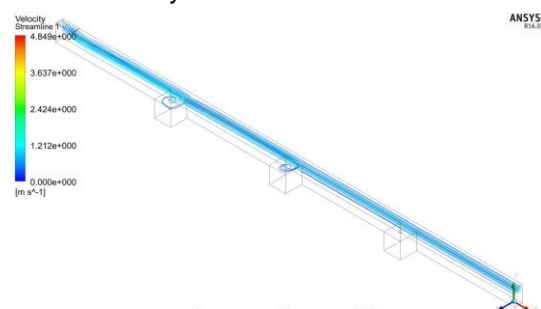


Fig. 8: Air streamlines for $Q_w: 3\text{m}^3/\text{h}$

V. RESULTS – COMPARISON

The numerical results are compared with the experimental data for the same operating conditions. In Figure 9 the comparison between the experimental and the numerical results for the 1m³/h water flow is presented. The higher separation values are achieved in low air flow rates (velocities).

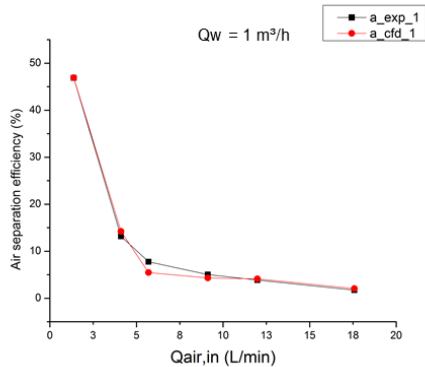


Fig. 9: Experimental and numerical comparison of α (%) – $Q_w: 1 \text{ m}^3/\text{h}$

In Figure 2 a significant difference between the numerical and the experimental value is observed for low air flow rate. The rest values for each air-water set export the same separating efficiency.

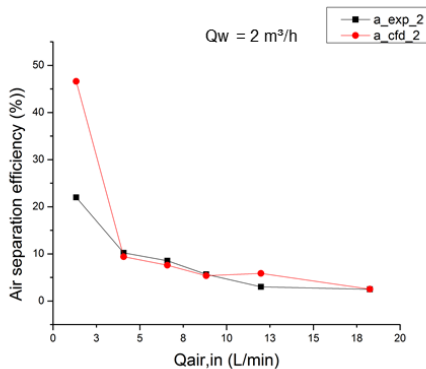


Fig. 10: Experimental and numerical comparison of α (%) – $Q_w: 2 \text{ m}^3/\text{h}$

In the last case where the water volume flow rate is 3m³/h the distribution of the results is almost the same. At the lowest air velocity, the numerical value is higher than the experimental one. The rest results are in the same range.

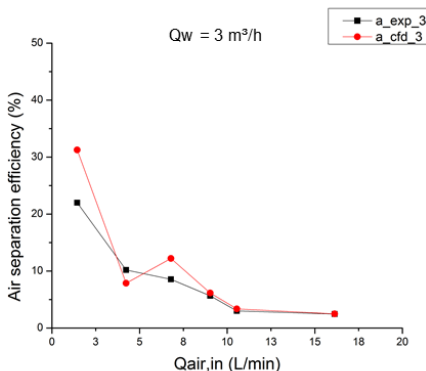


Fig. 11: Experimental and numerical comparison of α (%) – $Q_w: 3 \text{ m}^3/\text{h}$

VI. FLOW PATTERNS

The summary of the separation efficiency values (α) as well as the comparison of the flow patterns is presented in Table I, II and III for superficial water velocities 0.2, 0.4 and 0.6 relatively.

TABLE I: SUMMARY OF EXPERIMENTAL AND NUMERICAL SEPARATION EFFICIENCY AND FLOW PATTERNS

Water velocity: 0.2 m/s				
Air velocity (m/s)	Experimental Flow pattern	CFD flow pattern	α_{exp} (%)	α_{CFD} (%)
0.3	Stratified	Stratified	40.9	46.9
0.8	Wavy	Wavy	13.2	14.2
1.2	Wavy	Wavy	7.8	5.5
1.8	Wavy-Bubble	Wavy-Bubble	5.0	4.3
2.4	Stratified-Bubble	Stratified-Wavy	3.8	4.1
3.6	Stratified-Annular	Stratified-Annular	1.7	2.1

In Figure 9 the separation efficiency when the $J_w = 0.2 \text{ m/s}$ is the maximum when both the liquid and the air phase have the lowest volume rate values. The flow patterns and their characteristic formations are presented in Figure 12, taken from [16] and a brief explanation of the flow patterns is following:

Stratified Flow

The interaction between the two phases is rare and a smooth interface is established. Due to the gravitational forces that govern this regime the liquid and the gas phases flowed at the bottom and top of the duct respectively.

Bubble Flow

The bubbles are dispersed in the continuous liquid phase. In the current horizontal flow, the bubbles tend to congregate near to the top surface of the pipe.

Stratified Wavy Flow

As long as the velocity is increased in the stratified flow, waves are formed on the liquid-gas interface giving as a result the stratified wavy flow regime.

Slug Flow

In this pattern the liquid phase is continuous but inside the liquid there are large air bubbles. The presence of these bubbles often causes problems in applications and the prediction of slug flow is important.

Plug Flow

The characteristic bullet shapes are observed at the top of the tube and towards the upper surface of the cavities.

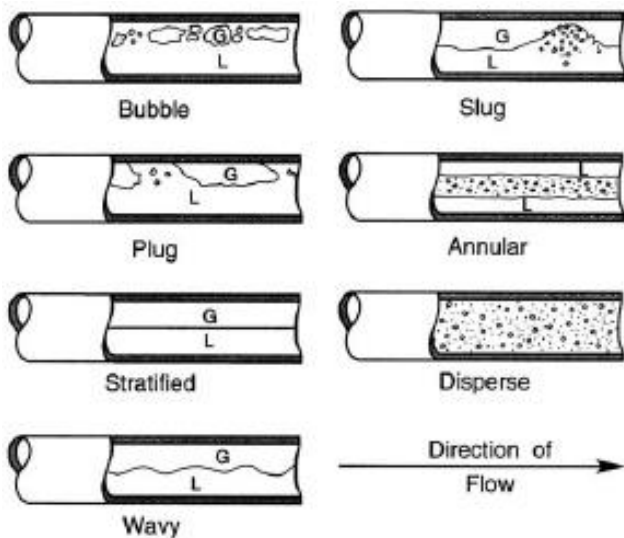


Fig. 12: Air water mixture horizontal flow patterns [16].

In Table II the flow patterns and the separation efficiency for the second case (J_w : 0.4 m/s) are listed. The flow is stratified when the velocities are low. As the volume rate is increased small bubbles transport inside the fluid.

TABLE II: SUMMARY OF EXPERIMENTAL AND NUMERICAL SEPARATION EFFICIENCY AND FLOW PATTERNS

Water velocity: 0.4 m/s				
Air velocity (m/s)	Experimental Flow pattern	CFD flow pattern	α_{exp} (%)	α_{CFD} (%)
0.3	Stratified	Stratified	22.0	46.6
0.8	Stratified-Bubble	Stratified-Bubble	10.2	9.4
1.3	Wavy-Bubble	Stratified-Bubble	8.5	12.2
1.8	Wavy-Bubble	Wavy-Bubble	5.7	6.1
2.4	Wavy-Bubble	Wavy-Bubble	3.0	3.4
3.6	Wavy-Annular	Stratified-Plug	2.5	2.5

Finally, as the air volume rate is higher, small waves are created at the interface of the two phases and in some cases the annular and the plug patterns are observed. The results of the last examined volume flow rate (J_w : 0.6 m/s) are listed in Table III. The flow at the beginning of the experiment/simulation is stratified. As the two superficial velocities are increased bubble flow, wavy flow and their combinations are observed. It must be mentioned that the best separation efficiency is achieved again for the lowest volume rates.

TABLE III: SUMMARY OF EXPERIMENTAL AND NUMERICAL SEPARATION EFFICIENCY AND FLOW PATTERNS

Water velocity: 0.6 m/s				
Air velocity (m/s)	Experimental Flow pattern	CFD flow pattern	α_{exp} (%)	α_{CFD} (%)
0.3	Stratified	Stratified	22.1	31.3
0.9	Bubble-Stratified	Bubble-Stratified	10.1	7.9
1.4	Wavy-Bubble	Stratified-Bubble-Wavy	8.3	12.2
1.8	Wavy-Bubble	Bubble-Stratified	5.6	6.1
2.1	Wavy-Bubble	Bubble-Stratified	3.3	3.4
3.3	Wavy-Bubble	Bubble-Stratified	2.4	2.5

VII. CONCLUSION

In this study the results and the validation of a CFD investigation compared to a previous experimental study [8] are presented. The numerical and the experimental results show very good convergence when the same operating conditions were applied to Fluent. The main conclusion of this study is that the mixture cavity separator can efficiently separate two phases of different densities without energy cost interventions. Secondly, when the specific idea is used for mixture separation in horizontal flow, the superficial velocities should be low to obtain stratified flow pattern. In this study the maximum separation efficiencies were achieved for $J_g = 0.3$ m/s. The separation efficiency results are not so satisfying so some modifications will be examined in future studies.

ACKNOWLEDGMENT

The present work was financially supported by the «Andreas Mentzelopoulos Scholarships University of Patras».

REFERENCES

- [1] L. Yang, B.J. Azzopardi and A. Belghazi, Phase separation of Liquid-Liquid Two-Phase Flow at a T-Junction, *AIChE Journal*, Vol. 52, No 1, pp 141-149, 2006.
- [2] D. Margaris (2007), "T-junction separation modelling in gas-liquid two phase flow", *Chemical Engineering and Processing*, Vol. 46, pp. 150-158.
- [3] Das G., Das P.K. and Azzopardi B.J. (2005), "The split of stratified gas-liquid flow at a small diameter T-junction", *International Journal of Multiphase Flow*, Vol. 31, pp. 514-528.
- [4] T. Stacey, B.J. Azzopardi, G. Conte (2000), "The split of annular two-phase flow at a small diameter T-junction", *International Journal of Multiphase Flow*, Vol. 26, pp. 845-856.
- [5] Emerson dos Reis, Leonardo Goldstein Jr. (2013), "Fluid dynamics of horizontal air-water slug flows through a dividing T-junction", *International Journal of Multiphase Flow*, Vol. 50, pp. 58-70.

[6] Chen Jian-lei, He Li-min, LUO Xiao-ming, BAI Hai-tao and WEI Yan-hai. (2012), "Simulation of oil-water two phase flow and separation behaviors in combined T-junctions", *Journal of Hydrodynamics*, Vol 24(6), pp. 848-857.

[7] Wang Li-yang, Wu Ying-xiang, Zheng Zhi-chu, Guo Jun, Zhang Jun, Tang Chi (2008), "Oil-water two-phase flow inside T-Junction", *Journal of Hydrodynamics*, Vol. 20, pp. 147-153.

[8] Zoga, D.A., Georgakis-Gavrilis, D.S., Margaris D.P. (2014), "Experimental investigation of a two-phase (Air-water) flow in a pipe with street canyon cavities", *International Review of Mechanical Engineering*, Vol 8, n. 6, pp. 1149-1155.

[9] Vardoulakis S., Fisher B., (2003), Perikleous K., Gonzalez-Flesca N., Modelling, Air Quality in Street Canyons: a Review, *Atmospheric environment*, Vol. 37, pp. 155-182.

[10] Panopoulos A. N., Margaris P. D., Kostakontis M. G., Styliaras E. P. (2015), "Numerical and Experimental Investigation of Air-Water Two-Phase Flow in a Pipe with Three Cavities of Different Aspect Ratios", *International Review of Mechanical Engineering*, Vol. 9, n. 2, pp. 145-153.

[11] Panopoulos A. Nikolaos and Margaris P. Dionissios (2015), "Numerical analysis of air-water separation in orthogonal pipe with parametrical outlet position", *6th International Conference on Experiments /Process /System /Modelling /Simulation /Optimization*, Athens.

[12] Panopoulos A. Nikolaos, Margaris P. Dionissios, Kapetanakis K. Markos and Zagklis-Tyraskis K. (2014), "CFD simulation of street canyon phenomenon as gas-liquid two-phase flow separation mechanism", *6th International Conference from "Scientific Computing to Computational Engineering*, Athens.

[13] Panopoulos A. Nikolaos, Margaris P. Dionissios, Charalambous A. Yiangos and Pipis P. Haris, (2015), "Experimental Study of Two Phase Flow in a new proposed orthogonal mixture separator", *International Review of Mechanical Engineering (I.RE.M.E.)*, Vol. 9, N. 6, pp. 561-567.

[14] Fluent Inc., *Fluent 15 Documentation-User's Guide*, 2013

[15] Koutsourakis N., (2010), "Flow and Pollutant Dispersion in Street Canyons: A Review", *Tech. Chron. Sci. J. TCG*, I, No 1.

[16] Weisman, J., Two phase patterns, Chapters 15 in *Handbook of Fluids in Motion*, Ann Arbor Science Publ., 409-425, 1983.